

1 **Impacts of anthropogenic emissions and cold air pools on urban to montane gradients**
2 **of snowpack ion concentrations in the Wasatch Mountains, Utah**

3
4 Steven J. Hall*¹, Gregory Maurer^{1,2}, Sebastian W. Hoch³, Raili Taylor^{4,5}, David R. Bowling^{1,2}

5
6
7 ¹Global Change and Sustainability Center, University of Utah

8 ²Department of Biology, University of Utah

9 ³Department of Atmospheric Sciences, University of Utah

10 ⁴Energy and Geoscience Institute, University of Utah

11 ⁵Department of Chemical Engineering, University of Utah

12
13
14 *Contact information for corresponding author:

15 steven.j.hall@utah.edu

16 608-886-6752

17 257 S, 1400 E, Room 201

18 Salt Lake City, UT 84112-0840

24 **Abstract**

25 Urban montane valleys are often characterized by periodic wintertime temperature
 26 inversions (cold air pools) that increase atmospheric particulate matter concentrations,
 27 potentially stimulating the deposition of major ions to these snow-covered ecosystems. We
 28 assessed spatial and temporal patterns of ion concentrations in snow across urban to montane
 29 gradients in Salt Lake City, Utah, USA, and the adjacent Wasatch Mountains during January
 30 2011, a period of several persistent cold air pools. Ion concentrations in fresh snow samples were
 31 greatest in urban sites, and were lower by factors of 4 – 130 in a remote high-elevation montane
 32 site. Adjacent undeveloped canyons experienced significant incursions of particulate-rich urban
 33 air during stable atmospheric conditions, where snow ion concentrations were lower but not
 34 significantly different from urban sites. Surface snow ion concentrations on elevation transects in
 35 and adjacent to Salt Lake City varied with temporal and spatial trends in aerosol concentrations,
 36 increasing following exposure to particulate-rich air as cold air pools developed, and peaking at
 37 intermediate elevations (1500 – 1600 m above sea level, or 200 – 300 m above the valley floor).
 38 Elevation trends in ion concentrations, especially NH_4^+ and NO_3^- , corresponded with patterns of
 39 aerosol exposure inferred from laser ceilometer data, suggesting that high particulate matter
 40 concentrations stimulated fog or dry ion deposition to snow-covered surfaces at the top of the
 41 cold air pools. Fog/dry deposition inputs were similar to wet deposition at mid-elevation
 42 montane sites, but appeared negligible at lower and higher-elevation sites. Overall, snow ion
 43 concentrations in our urban and adjacent montane sites exceeded many values reported from
 44 urban precipitation in North America, and greatly exceeded those reported for remote
 45 snowpacks. Sodium, Cl^- , NH_4^+ , and NO_3^- concentrations in fresh snow were high relative to
 46 previously measured urban precipitation, with means of 120, 117, 42, and 39 $\mu\text{eq l}^{-1}$,

47 respectively. After exposure to atmospheric particulate matter during cold pool events, surface
 48 snow concentrations peaked at 2500, 3600, 93, and 90 $\mu\text{eq l}^{-1}$ for these ions. Median nitrogen (N)
 49 deposition in fresh urban snow samples measured 0.8 kg N ha⁻¹ during January 2011, with
 50 similar fog/dry deposition inputs at mid-elevation montane sites. Wintertime anthropogenic air
 51 pollution represents a significant source of ions to snow-covered ecosystems proximate to urban
 52 montane areas, with important implications for ecosystem function.

53
 54 **Key words:** inversion, montane, nitrogen deposition, PM_{2.5}, snow chemistry, urban

56 1. Introduction

57 Snow represents the dominant form of precipitation in many arid montane regions and
 58 provides a primary source of nutrient ions to ecosystems, with potentially detrimental impacts on
 59 water quality and ecosystem function when ion inputs are enhanced by anthropogenic emissions
 60 (Lewis et al. 1983, Cerling and Alexander 1987, Jeffries 1990, Williams and Tonnessen 2000).
 61 In particular, nitrogen (N) inputs from atmospheric deposition can contribute to undesired
 62 increases in productivity, species changes, and aquatic eutrophication, especially in seasonally
 63 snow-covered environments where nutrients rapidly elute during melting (Jeffries 1990,
 64 Williams and Tonnessen 2000, Baron et al. 2011). Many studies of snow chemical composition
 65 over the past three decades have explicitly avoided measurements of urban emission hot-spots
 66 (Jeffries 1990, Nickus et al. 1997), instead focusing on remote wilderness sites (Williams and
 67 Melack 1991, Pomeroy et al. 1999, Kang et al. 2004, Williams et al. 2009). Cities often exhibit
 68 higher ion concentrations and fluxes in rainfall and dry deposition relative to adjacent areas, with
 69 trends varying among chemical species (e.g. Lewis et al. 1984, Gatz 1991, Fenn et al. 2003).

70 However, urban ion deposition studies have typically focused on summer rainfall (Lovett et al.
 71 2000, Bettez and Groffman 2013, Rao et al. in press), and very few comprehensive
 72 measurements of snow ions have been reported in urban environments (Lewis et al. 1983). Little
 73 is known about spatial and temporal variation in ion deposition to snow across urban to rural
 74 gradients, and whether snow ion concentrations vary systematically with urban proximity as
 75 observed for rainfall. Even less is known about temporal couplings between urban air pollution
 76 events and ion inputs to snow. These patterns may be critical for understanding and predicting
 77 nutrient inputs to seasonally snow-covered ecosystems.

78 Wintertime meteorological characteristics of urbanized montane valleys have the
 79 potential to significantly increase snowpack ion loading in wet, dry, and cloud deposition. High
 80 pressure events persisting for days to weeks often stabilize cold air pools, trapping local
 81 anthropogenic emissions, and leading to the accumulation of ion-rich primary and secondary fine
 82 particulate matter (PM 2.5) in the atmosphere (Silcox et al. 2012, Kelly et al. 2013, Lareau et al.
 83 2013, Whiteman et al., 2014). These conditions prevail in many rapidly growing metropolitan
 84 areas in the Western United States (e.g. Salt Lake City, Utah; Boise, Idaho; Reno, Nevada) and
 85 physiographically similar regions worldwide (e.g. Santiago, Chile; Chen et al. 2012, Cereceda-
 86 Balic et al. 2012). Cold air pools associated with elevated PM 2.5 also occur in non-mountainous
 87 regions over shorter timescales (Wallace and Kanaroglou 2009), and could thus represent a
 88 widely important phenomenon for wintertime urban ion deposition.

89 Empirical studies linking atmospheric aerosol concentrations with ion deposition remain
 90 uncommon, especially for snow (Yalcin et al. 2006, Dolislager et al. 2012). Ammonium nitrate
 91 and ammonium sulfate originating from anthropogenic precursors—ammonia, nitrogen oxides,
 92 and sulfur dioxide—comprise the majority of PM 2.5 in many urban areas (Connell et al. 2006,

93 Hand et al. 2012, Kelly et al. 2013). The impact of urban atmospheric emissions and particulate
 94 matter on snowpack ion loading is largely unknown, but Cerling and Alexander (1987)
 95 documented extremely high concentrations of ions in rime and snow at sites in and adjacent to
 96 Salt Lake City during a prolonged cold air pool in 1985. Dry and fog deposition of gases and
 97 particles to snow-covered surfaces have previously been shown to comprise relatively minor
 98 sources of ions in comparison with snowfall (Bergin et al. 1995, Björkman et al., 2013). Rather,
 99 net losses of NO_3^- from the snowpack between precipitation events can be significant (Williams
 100 and Melack 1991, Pomeroy et al. 1999, Williams et al. 2009). However, this subject has received
 101 little attention in urban environments, where elevated aerosol concentrations during cold air
 102 pools could enhance dry or cloud deposition in addition to wet deposition, and yield ecologically
 103 significant fluxes of ions to the snowpack.

104 Here, we assessed spatial and temporal patterns of ion concentrations in bulk snow and
 105 snow surface samples across urban to montane gradients in Salt Lake City, Utah, USA, and the
 106 adjacent Wasatch Mountains. This major metropolitan area experiences frequent wintertime
 107 atmospheric temperature inversions that promote particulate matter accumulation over time,
 108 yielding PM 2.5 concentrations that routinely violate national ambient air quality standards
 109 (Silcox et al. 2012, Kelly et al. 2013, Whiteman et al. 2014). We demonstrated that urban air
 110 pollution associated with cold air pools significantly affected spatial and temporal patterns of
 111 snow ion concentrations, with implications for water quality and ecosystem function.

113 2. Methods

114 2.1 Sampling locations

115 We sampled ion concentrations of snow collected in the Salt Lake City, UT, USA
 116 metropolitan area and the adjacent Wasatch Mountains (Fig. 1) during December 2010 – January
 117 2011, including multiple persistent cold air pools (PCAPS) described in an intensive atmospheric
 118 observational study by the same name (Lareau et al. 2013). Sampling locations spanned urban
 119 Salt Lake City and adjacent montane ecosystems to assess variation in snow chemical
 120 composition with landscape position, elevation, and time. We collected two distinct types of
 121 samples: bulk snow and surface snow. Sampling elevations are expressed in meters above sea
 122 level; the valley floor has an approximate elevation of 1300 m.

123 *2.2 Bulk snow samples*

124 We sampled fresh bulk snow samples at three urban sites and along two elevation
 125 gradients in adjacent montane canyons (Fig. 1). Urban sites comprised a roof on the University
 126 of Utah campus, a residential yard, and an elementary school. The two montane canyons, Red
 127 Butte and Big Cottonwood, experienced elevated particulate matter concentrations during cold
 128 air pools (Fig. 2). Red Butte Canyon is a Research Natural Area managed by the USDA Forest
 129 Service with restricted access and minimal vehicle traffic. Big Cottonwood Canyon contains a
 130 highway and two major ski resorts. We sampled each canyon at elevations of
 131 approximately 1600, 1800, and 2000 m, respectively. We also sampled an additional very high
 132 elevation site (2900 m) above Big Cottonwood Canyon. Sites were sampled 5 – 7 times between
 133 December 17, 2010 and January 30, 2011 (total n = 51 bulk snow samples).

134 Bulk snow samples were collected on rigid high-density polyethylene (HDPE) sampling
 135 surfaces mounted on white plywood (0.6 x 0.6 m) with a 2 m vertical pole (hereafter termed
 136 “stormboards”, n = 10), deployed in the field for the entire study period. Stormboards were
 137 located in undisturbed clearings and sampled within 24 – 48 hours after each snowfall by

138 vertically coring from the top of the snowpack to the HDPE surface with a 5.1 cm diameter PVC
 139 tube. Samples were quantitatively transferred to HDPE bottles by placing a plastic knife under
 140 the tube. Two samples were collected from each stormboard and composited. We removed
 141 remaining snow from stormboards following sampling and rinsed surfaces with deionized water.
 142 Stormboards were replaced on top of the snowpack in an adjacent undisturbed location. All
 143 sampling supplies were acid-washed and rinsed with deionized water before use, and clean nitrile
 144 gloves worn during sample collection. Field blanks were collected to assess contamination by
 145 rinsing sampling cores with deionized water in the field. Ion concentrations in field blanks
 146 represented < 3 % of mean snow concentrations for all ions except for K⁺ (~10 % of sample
 147 concentrations). This variation (3 %) only slightly exceeded the analytical uncertainty of ion
 148 analyses (assessed using the standard deviation of check standards). We calculated snow water
 149 equivalent for bulk snow samples by dividing snow sample mass by sampling area.

150 *2.3 Snow surface samples*

151 Snow surface samples were repeatedly collected from two elevation transects (total n =
 152 90 snow surface samples; Figs. 1 and 2). The urban transect was located on a south-facing slope
 153 in the Avenues neighborhood of Salt Lake City at the same seven sites described by Silcox et al.
 154 (2012). The montane transect was located on a west-facing ridge of Grandeur Peak, a mountain
 155 immediately East of Salt Lake City. This transect comprised 20 sampling sites located every 50
 156 meters in elevation from 1550 to 2500 m. Snow surface samples were collected from each site by
 157 scraping the mouth of a 60 ml HDPE bottle across the snow surface to a depth of approximately
 158 1 cm. The montane and urban transects were sampled four and five times, respectively, during
 159 January 2011.

160 *2.4 Chemical analyses*

161 Thawed samples were vacuum filtered through pre-rinsed Whatman Nuclepore 1.0 μm
 162 membranes and analyzed for major anions (Cl^- , SO_4^{2-} , NO_3^-) by ion chromatography and cations
 163 (Na^+ , Ca^{2+} , NH_4^+ , Mg^{2+} , K^+) by atomic absorption spectrometry at the Kiowa Environmental
 164 Chemistry Laboratory at the University of Colorado, as described in Williams et al. (2009).
 165 Detection limits for all analytes reported here were $< 0.5 \mu\text{eq l}^{-1}$, with analytical precision $< 2 \%$.
 166 A subset of samples ($n = 33$) was also analyzed for acid neutralizing capacity (ANC) and pH to
 167 calculate charge balance (carbonate species were assessed indirectly via ANC). Most samples
 168 had a small excess positive charge with a median ion percent difference (difference of anion
 169 charge and cation charge divided by their total) of -8% . Unmeasured anions including organic
 170 acids, nitrite, and fluoride likely accounted for this discrepancy.

171 *2.5 Meteorological and air-quality measurements*

172 Concentrations of PM 2.5 were measured hourly by the Utah Department of
 173 Environmental Quality at a site co-located with the lowest elevation on our urban transect
 174 (Figure 1; data available at <http://www.airmonitoring.utah.gov/dataarchive/archpm25.htm>). We
 175 compared temporal relationships between PM 2.5 concentrations and ion concentrations in
 176 surface snow samples. For each sample, we integrated hourly PM 2.5 concentrations from the
 177 previous snowstorm until the time of sampling as a metric of potential exposure to PM2.5,
 178 irrespective of elevation. Snow accumulation at the mouth of Little Cottonwood Canyon was
 179 recorded daily. Near-surface air temperatures were measured along a pseudo-vertical transect (50
 180 m elevation contours) on the montane transect with sensors (Hobo Pro, Onset Computer
 181 Corporation, MA) mounted on fence posts at ~ 1.2 m height; we report mean temperature profiles
 182 from several days to illustrate contrasting atmospheric conditions during cold air pool
 183 development.

184 *2.6 Aerosol exposure index*

185 We recorded aerosol backscatter profiles with a Vaisala CL31 laser ceilometer located at
 186 the center of the Salt Lake Basin (Fig. 1). An index for exposure of the surface snow to aerosol
 187 loading from the adjacent atmosphere was derived as the time integral of the backscatter
 188 coefficient β between the last snowfall and the sampling time. As the \log_{10} of β yields negative
 189 numbers and -8 can be considered the minimum value for $\log_{10} \beta$, we added 8.0 to backscatter
 190 data to achieve a positive scale for integrated exposure. This metric implies that higher exposure
 191 occurs at elevations where the atmosphere exhibited the largest values of aerosol backscatter for
 192 the longest time. Backscatter represents a semi-quantitative measure of aerosol abundance that is
 193 not directly proportional to concentrations of a single aerosol species, as backscatter depends on
 194 particle size and composition. Both the backscatter coefficient in Fig. 5 and the aerosol exposure
 195 index (Fig. 7) thus represent semi-quantitative approximations of aerosol concentrations or
 196 exposure.

 197 *2.7 Statistical analysis*

198 We used ANOVA and linear mixed effects models to evaluate spatial and temporal
 199 differences in ion concentrations among sites and dates. Ion concentration data were log-
 200 transformed to reduce heteroscedasticity. For bulk snow samples, we compared ion
 201 concentrations among sites over the entire sampling period using ANOVA. For surface snow
 202 samples, we fit two separate models for each ion. First, we assessed differences among sampling
 203 dates irrespective of elevation, including random effects for sites to account for repeated
 204 sampling. Pairwise differences among dates were evaluated with Tukey comparisons. Secondly,
 205 we fit models including sampling date, elevation, and elevation x date interactions as fixed
 206 effects, and sampling sites as random effects. Ion concentrations displayed strong nonlinear

207 trends with elevation for one sampling date (January 28) in the urban transect, so we fit
 208 regression models including a quadratic term for this date. We fit all models using the lm or lme
 209 functions in R (Pinheiro et al. 2013).

210

211 **3. Results and Discussion**

212 *3.1 Bulk snow ion concentrations*

213 Concentrations of major ions varied by up to four orders of magnitude among bulk
 214 stormboard snow samples and showed significant spatial variation from urban to montane sites.
 215 Sodium and Cl^{-1} had the highest concentrations in bulk and surface snow samples, followed by
 216 Ca^{2+} , NH_4^{+} , NO_3^{-} , SO_4^{2-} , Mg^{2+} , and K^{+} , respectively (Fig. 3). Ion concentrations in bulk snow
 217 samples decreased significantly with elevation from the urban sites to the very high elevation Big
 218 Cottonwood Canyon site for all species except for K^{+} , whereas sites in Big Cottonwood and Red
 219 Butte Canyons were typically intermediate and not significantly different. (Fig. 3). Mean
 220 concentrations of ions in the urban samples relative to the very high elevation site were greater
 221 by factors of 130 (Cl^{-1}), 31 (Na^{+}), 8 (Ca^{2+}), 12 (NH_4^{+}), 8 (NO_3^{-}), 8 (SO_4^{2-}), 11 (Mg^{2+}), and 4 (K^{+}).
 222 Proton concentrations did not differ among sites ($7.4 \pm 1.1 \mu\text{eq l}^{-1}$, $n = 40$), and were equivalent
 223 to $\text{pH } 5.13 \pm 0.07$.

224 Despite variation in ion concentrations between the urban and canyon sites, ion mass
 225 loading appeared similar across the landscape due to weak inverse relationships between snow
 226 water equivalent and ion concentrations (Fig. A1 and A2). These patterns suggest that increasing
 227 snow water equivalent with elevation due to orographic precipitation may be as important as
 228 spatial variation in ion concentrations in controlling ion mass fluxes. However, we note that
 229 estimates of ion mass loading, as opposed to ion concentrations, are inherently imprecise in

230 montane environments due to spatial heterogeneity in snow water equivalent, which our study
 231 was not designed to assess (Molotch and Bales 2005). Furthermore, snow ion concentrations are
 232 especially relevant to biological processes in open systems due to the fundamental dependence of
 233 nutrient uptake rates and osmotic relations on ion concentration gradients, as opposed to ion
 234 mass fluxes.

235 *3.2 Pairwise correlations among major ions*

236 Almost all ion pairs exhibited significant positive correlations except for H^+ (Table 2),
 237 indicating coherence in distinct sources of these ions. Notably, correlations among ions tended to
 238 be substantially weaker in the surface snow samples relative to the bulk snow samples,
 239 suggesting a mixture of different sources and/or depositional processes (wet + dry + fog). One
 240 exception was the strong correlation between Ca^{2+} and SO_4^{2-} in surface snow, likely reflecting
 241 gypsum dust from nearby salt flats. Sodium and Cl^- had the strongest possible correlation ($r = 1$)
 242 in both the bulk and surface snow samples, strongly implicating NaCl aerosol inputs. The next
 243 strongest correlations were between NH_4^+ , SO_4^{2-} , and NO_3^- , likely reflecting inputs of particulate
 244 $(NH_4)_2SO_4$ and NH_4NO_3 , which frequently represent dominant constituents of PM 2.5 in this
 245 region and nationwide (Hand et al. 2012, Kelly et al. 2013). Calcium and Mg^{2+} (but not K^+) also
 246 scaled closely, potentially indicating a common source in carbonate dust or ash (Lajtha and
 247 Jones, 2013).

248 *3.3 Comparisons of snow ion concentrations with previous studies*

249 Concentrations of NH_4^+ , NO_3^- , Na^+ , and Cl^- in the urban samples were several times
 250 greater than previous measurements in snow from regions with similar climate and physiography
 251 (Table 1). Sodium and Cl^- were the dominant ions across all sites. The high concentrations of
 252 Na^+ and Cl^- (tens – hundreds of $\mu eq\ l^{-1}$) we observed in our urban sites were similar to those

253 documented in snow in Montreal, Canada, which were likely derived from road deicing salt
 254 aerosols (Lewis et al. 1983). The highly saline margins of the Great Salt Lake may contribute to
 255 high background Na^+ and Cl^- evident in the canyon and remote sites compared with other
 256 montane snow studies (Table 1). Our urban bulk snow Na^+ and Cl^- concentrations were
 257 comparable to mean precipitation measurements in maritime regions such as Athens, Greece
 258 ($\sim 90 \mu\text{eq l}^{-1}$), and slightly greater than Los Angeles, California ($\sim 45 \mu\text{eq l}^{-1}$; Gatz 1991),
 259 suggesting high background inputs from lake-derived aerosols in addition to episodic road salt
 260 additions. Anthropogenic sources likely contributed to the sporadic occurrence of extremely high
 261 NaCl at some sites (discussed below).

262 Concentrations of NH_4^+ and NO_3^- in Salt Lake City snow were generally greater than
 263 those in rainfall from other North American cities, and from one other study that measured urban
 264 snow ion concentrations. We acknowledge that substantial spatial and temporal variability exists
 265 within cities and among calibrations and analytical methods used in the studies reported here, but
 266 we provide mean values from other studies to facilitate general comparisons, irrespective of their
 267 possible statistical significance. We found four-fold greater concentrations of NH_4^+ , similar NO_3^-
 268 , and much lower SO_4^{2-} as compared with snow from urban Montreal measured in the early
 269 1980's (Table 1; Lewis et al. 1983). Our urban bulk snow typically had greater NH_4^+
 270 concentrations than mean wet precipitation measured in Detroit, Chicago, Los Angeles, and New
 271 York City in the 1980's (approximately 26, 35, 20, and 15 $\mu\text{eq l}^{-1}$ for each city, respectively), as
 272 well as greater NO_3^- concentrations than these cities (approximately 36, 32, 31, and 27 $\mu\text{eq l}^{-1}$,
 273 respectively; Gatz 1991). Urban snow NO_3^- concentrations were similar to those of bulk summer
 274 rain precipitation measured in downtown New York City in 1996 ($\sim 40 \mu\text{eq l}^{-1}$), but our NH_4^+
 275 concentrations were substantially greater than the 25 $\mu\text{eq l}^{-1}$ measured there (Lovett et al. 2000).

276 Our urban snow also had greater NH_4^+ and NO_3^- concentrations compared with most recent
 277 precipitation samples (2008 – 2010, rain and snow) in National Atmospheric Deposition
 278 Program (NADP) sites documented in a meta-analysis, which typically measured $< 25 \mu\text{eq l}^{-1}$
 279 (Lajtha and Jones 2013). These sites were explicitly located to minimize the direct influence of
 280 urban sources. Salt Lake City snow NH_4^+ and NO_3^- concentrations were similar to several
 281 European Monitoring and Evaluation Programme sites reported in this study (ibid.).

282 *3.4 Air quality dynamics during the snow sampling period*

283 Daily mean PM 2.5 concentrations at the Salt Lake Valley floor varied between 10 – 70
 284 $\mu\text{g m}^{-3}$ during January 2010 (Fig. 4) concomitant with cold air pool dynamics (Lareau et al.
 285 2013). Three distinct cold air pool episodes of Jan 1 – 9, 12 – 16, and 26 – 31 are visible in Fig. 4
 286 as periods of increased PM 2.5 surface concentrations. Aerosol backscatter increased during
 287 these cold air pool episodes when mixing was inhibited by stable stratification in the atmosphere
 288 (Fig. 5). The height of the aerosol layer varied in response to changing meteorological
 289 conditions, with the top typically positioned between 1500 – 2000 masl. When fog or a low
 290 stratus cloud deck formed, the ceilometer laser beam was occasionally completely attenuated.
 291 This led to signal saturation and elimination of returns above the fog/cloud layer during the
 292 nights between January 6 – 8, and between January 27 – 30.

293 *3.5 Temporal variation in surface snow ion concentrations*

294 Surface snow samples from the urban and montane elevation transects exhibited
 295 significant temporal variation in ion concentrations approximately proportional to cold air pool
 296 development and time-integrated PM 2.5 concentrations measured on the valley floor (Fig. 4).
 297 Irrespective of elevation, ion concentrations in the montane transect were significantly greater on
 298 either Jan 7, or both Jan 7 and 30 as compared with Jan 14 and 24 for several ions (Cl^- , Na^+ ,

299 Ca^{2+} , K^{+} ; Fig. 4). The dates with significantly greater snow surface ion concentrations coincided
 300 with periods of greater time-integrated PM 2.5 exposure, calculated by multiplying valley
 301 surface PM 2.5 concentrations by time between snow events (indicated by the size of shaded
 302 regions in Fig. 4). On Jan 7 and 30, time-integrated PM 2.5 exposure reached 4760 and 3070 μg
 303 m^{-3} hr, whereas the dates with significantly lower surface ion concentrations (Jan 14 and 24) had
 304 much lower PM 2.5 exposure (930 and 300 $\mu\text{g m}^{-3}$ hr). In the urban transect, concentrations of
 305 Ca^{2+} , NO_3^- , and SO_4^{2-} were significantly greater on Jan 28 than on the other sampling dates,
 306 coinciding with a PM 2.5 exposure of 1340 $\mu\text{g m}^{-3}$ hr. The other sampling dates (Jan 5, 14, 24,
 307 and 26) had lower PM 2.5 exposures of 1090, 930, 300, and 350 $\mu\text{g m}^{-3}$ hr, respectively.

308 The potential influence of road salt on surface snow Na^{+} and Cl^{-} was especially evident in
 309 the montane samples on Jan 7, when concentrations increased by an order of magnitude to
 310 thousands of μeq^{-1} between 1600 – 1800 m (Fig. 6). High deposition of Na^{+} and Cl^{-} to the
 311 montane transect could have been generated by a combination of road salt application and high-
 312 speed vehicle traffic on Interstate Highways 80 and 215, which are located within several
 313 hundred meters of the lower sites (Fig. 1); the urban elevation transect was not located with
 314 similar proximity to major highways.

315 *3.6 Variation in surface snow ion concentrations and particulate matter with elevation*

316 Elevational trends in surface snow ion concentrations differed between the urban and
 317 montane transects (Fig. 6). On the montane transect, ion concentrations consistently decreased
 318 with elevation ($p < 0.0001$) by a relationship that varied among sampling dates ($p < 0.0001$,
 319 elevation x date interaction). Samples collected on January 7 and 30, during cold air pools with
 320 greatest PM 2.5 exposure, exhibited the greatest elevational differences along the transect (Fig.
 321 6). In the urban transect, significant linear trends were evident only for Na^{+} and Cl^{-} , which

322 decreased with increasing elevation ($p < 0.05$ for elevation and elevation x date interaction).
 323 However, several ions in the urban transect exhibited increasingly nonlinear concentration trends
 324 with elevation during the development of a prominent temperature inversion between January 24
 325 – 30 (Figs. 5-7). On January 24 and 26, the daily mean temperature profile showed a temperature
 326 decrease with height approximately following a lapse rate of $5.5 \text{ }^\circ\text{C km}^{-1}$, corresponding with a
 327 nearly uniform elevational aerosol exposure profile indicated by ceilometer backscatter (Fig. 7).
 328 During these dates, surface snow NH_4^+ and NO_3^- concentrations varied little with elevation,
 329 although a subtle trend of increasing NH_4^+ with decreasing elevation was evident in both
 330 transects. However, by January 28 and 30, a cold pool developed with a strong elevated
 331 temperature inversion layer between 1600 – 2000 masl. Peak aerosol exposure occurred between
 332 1500 – 1600 masl corresponding with the vertical structure of this cold air pool (Fig. 7). The two
 333 other cold air pools during January 2011 showed similar trends, although exposure peaked at
 334 slightly lower elevations (1400 – 1500 m; Fig. A3). Corresponding with increased aerosol
 335 exposure, concentrations of NH_4^+ began to increase at lower elevations on January 26, and by
 336 January 28, NH_4^+ and NO_3^- significantly peaked at approximately 1500 masl in the urban
 337 transect (Fig. 7; $p < 0.01$ and $p < 0.05$ for quadratic relationships with elevation, respectively).
 338 Similarly, by January 30, concentrations of these ions peaked in the montane transect at
 339 approximately 1600 masl.

340 Non-linear elevational trends in aerosol exposure and ion accumulation during cold air
 341 pool development are generally consistent with elevation trends in PM 2.5 concentrations
 342 measured by Silcox et al. (2012) on the montane transect, which peaked between 1350 – 1400 m
 343 on January 6 and 28. Subtle differences between elevational trends in PM 2.5 and our exposure
 344 index (Fig. 7), which peaked at slightly higher elevations, may have been due to the fact that the

345 ceilometer measured aerosols regardless of their diameter, whereas PM 2.5 measurements by
 346 definition are restricted to a fine subset of particulate matter ($< 2.5 \mu\text{m}$). These differences could
 347 also have been influenced by horizontal spatial variability in aerosol concentrations between the
 348 location of the ceilometer and the urban transect, although PM 2.5 concentrations measured at
 349 several sites within the Salt Lake Valley were very similar during Jan 2011 (Silcox et al. 2012).
 350 The improved correspondence between elevation trends in surface snow ions and our index of
 351 aerosol exposure, as opposed to elevation trends in PM 2.5, suggests that coarser aerosols (> 2.5
 352 μm) might represent an important source of ions to snow.

353 *3.7 Nitrogen deposition fluxes*

354 We cannot conclusively separate fog, hoar, rime, and/or dry deposition ion inputs
 355 (collectively termed “fog/dry deposition”) from wet snowfall, but can estimate their relative
 356 importance. Fresh bulk snow likely contains mostly wet ion deposition, but may also capture
 357 some fog/dry inputs deposited to the stormboard surface prior to snowfall. Bulk snow samples
 358 provide maximum estimates of wet deposition, whereas comparison of surface snow samples
 359 over time yields potential net fog/dry deposition. As a cold air pool developed between Jan 24
 360 and Jan 30, changes in surface snow NH_4^+ concentrations over time across the montane gradient
 361 varied between a decrease of $11 \mu\text{eq l}^{-1}$ and a maximum increase of $62 \mu\text{eq l}^{-1}$ at mid elevations
 362 (Fig. 7). Nitrate showed similar patterns, where concentrations increased between 0 and $70 \mu\text{eq l}^{-1}$
 363 over this period. The urban transect showed similar increases between Jan 24 and Jan 28 of 15
 364 $- 38$ and $29 - 56 \mu\text{eq l}^{-1}$ for NH_4^+ and NO_3^- , respectively. These trends reflect significant net
 365 positive fog/dry N deposition at mid-elevation sites, and negligible deposition or small net N
 366 losses at the low and high-elevation sites.

367 The highest rates of surface deposition in the montane and urban transects were
 368 equivalent to N fluxes of approximately 0.08 – 0.10 kg N ha⁻¹ for each species (NH₄⁺ and NO₃⁻)
 369 over these four and six-day periods. Maximum rates of fog/dry deposition at mid-elevation sites
 370 during the late January cold air pool were comparable to deposition from individual storm events
 371 (bulk snow samples) in the urban area, which had median values of 0.06 - 0.05 kg N ha⁻¹ for
 372 NH₄⁺ and NO₃⁻ (Fig. A2). The seven measured snow events in January 2011 deposited a total
 373 median N input of approximately 0.8 kg ha⁻¹, with a smaller additional contribution from fog/dry
 374 deposition that varied strongly with elevation. At mid-elevation (1400 – 1600 m) sites, fog/dry
 375 deposition may have deposited approximately 0.5 kg N ha⁻¹ over the three January cold air pools,
 376 if rates of snow surface N accumulation from January 24 - 30 are representative of the earlier
 377 cold air pools. At elevations less than 1400 and greater than 1800 m, however, net fog/dry
 378 deposition appeared to be much smaller.

379 *3.8 Implications for ecosystem function*

380 Baron et al. (2011) showed that N loading of several kg ha⁻¹ yr⁻¹ can represent an
 381 ecological critical load for nutrient enrichment in Western US montane ecosystems. Given that
 382 our median measured N deposition measured almost 1 kg ha⁻¹ in January 2011 alone, wintertime
 383 deposition can represent an ecologically relevant source of N to these urban and protected
 384 montane sites. Summertime N deposition remains to be measured in this region. If our data are
 385 representative of other cities, they have significant implications for quantifying N deposition to
 386 other urban ecosystems, given that wintertime data were absent from several previous urban
 387 deposition studies (Rao et al. In press, Lovett et al. 2000, Bettez and Groffman 2013).
 388 Wintertime N inputs have the potential to alter community structure and ecosystem function as

389 they are delivered to soils and streams during snowmelt (Jeffries 1990, Williams and Tonnessen
 390 2000, Williams et al. 2009, Baron et al. 2011).

391 Episodically high inputs yielding high aqueous concentrations of Na⁺ and Cl⁻ also have
 392 important ecological implications. Some aquatic organisms, including amphibians, are highly
 393 sensitive to elevated ion concentrations. Solution conductivities of 500 μS cm⁻¹ (equivalent to
 394 NaCl concentrations of several hundred μM) can decrease larval survival (Karraker et al. 2008).
 395 We found peak NaCl concentrations exceeding 3000 μM in surface snow on the montane
 396 transect (Fig. 6), likely derived from road salt aerosols. Snowpack-integrated NaCl
 397 concentrations are presumably lower than those found in surface snow, but ion concentrations in
 398 initial snowmelt increase as a consequence of preferential ion elution, and are likely to be of
 399 similar magnitude to those found detrimental for amphibian survival. Detailed relationships
 400 between snowpack and stream ion concentrations are beyond the scope of the present study. The
 401 canyons adjacent to the montane elevation transect are “protected” watersheds managed by the
 402 USDA Forest Service to maintain a clean drinking water supply for urban use and for
 403 conservation purposes. The Wasatch Mountains contain four large federally-designated
 404 wilderness areas. Nevertheless, our data show that they experience significant ion pollutant
 405 inputs as a consequence of their proximity to the urban Salt Lake Valley. High snow inputs of
 406 other ions such as Ca²⁺, Mg²⁺, and SO₄²⁻ are unlikely to have substantial ecological effects in this
 407 region given the prevalence of sedimentary parent material and high stream concentrations of
 408 these ions (S. Hall, unpublished data).

409 *3.9 Couplings between ion deposition and atmospheric particulate matter dynamics*

410 The qualitative correspondence between increased concentrations of major ions in surface
 411 snow (Fig. 6), elevational trends in atmospheric particulate matter (Figs. 5 and 7), and

412 differences in time-integrated PM 2.5 exposures following snowstorms (Fig. 4) all point to the
 413 importance of urban particulate matter deposition as a source of ions to snow in this region—a
 414 mechanism that has received scant attention in the literature (Cerling and Alexander 1987).
 415 Observed variation in surface snow ions between snow events could have been caused by dry
 416 deposition or by the precipitation of surface rime or snow grains from moisture originating
 417 within the cold air pool. Composition of PM 2.5 is typically dominated by the major ions,
 418 especially NH_4^+ , SO_4^{2-} , and NO_3^- (Hand et al. 2012), which are readily soluble in melted snow
 419 samples. Thus, variation in PM 2.5 concentrations in urban environments may represent an
 420 important proximate control on ion deposition to snow, especially at elevations where aerosol
 421 clouds are in close contact with the snow surface. The surface snow ion concentrations we
 422 observed were greater than those observed elsewhere in bulk snow, although they were
 423 substantially lower than previous measurements of rime and surface snow in the Salt Lake
 424 Valley (Table 1; Cerling and Alexander, 1987). These differences may reflect the partial success
 425 of emissions regulations in decreasing atmospheric particulates over this time period (Whiteman
 426 et al. 2014). Low particulate matter concentrations characteristic of remote montane regions may
 427 explain the absence of measurable dry ionic snowpack deposition reported in previous studies
 428 (Williams and Melack 1991, Pomeroy et al. 1999, Williams et al. 2009).

429 It is important to note that although our surface snow measurements focused on sites in
 430 close proximity to urban Salt Lake City, high concentrations of urban-derived particulate matter
 431 extended into significant portions of adjacent montane canyons (Fig. 2). For instance, vertical
 432 trends in aerosol distribution (Fig. 5) implied that low and mid-elevation canyon sites (Fig. 1)
 433 were exposed to urban aerosols for much of January 2011. Incursions of urban particulate matter
 434 (e.g., Fig. 2) may explain the absence of significant differences between bulk snow ion

435 concentrations in urban and canyon samples; the very high elevation site was situated well above
 436 the urban cold air mass (Figs. 1, 3). In fact, the peak in aerosol exposure that we observed at
 437 approximately 1600 m concomitant with increased NH_4^+ and NO_3^- concentrations implies that
 438 montane sites at intermediate elevation experience elevated dry/fog ion deposition relative to the
 439 urban valley floor, perhaps analogous to a “bathtub ring” of accumulated pollution at the top of
 440 cold air pools. The correspondence of elevated snow ions to elevations of maximum ceilometer
 441 attenuation suggests that aerosol clouds may have generated aerosol-rich rime on the snow
 442 surface. The hypothesis suggested by our data, that wintertime ion deposition peaks in montane
 443 environments at the top of cold air pools, merits further exploration.

444 4. Conclusions

445 We observed high concentrations of major ions in bulk snow and surface samples
 446 collected within and adjacent to Salt Lake City, UT, during a period of several cold air pools that
 447 generated increased concentrations of anthropogenic particulate matter in January 2011.
 448 Concentrations of Na^+ , Cl^- , NH_4^+ , and NO_3^- , in particular, were typically greater than those
 449 measured in other studies of urban precipitation, and concentrations far exceeded typical values
 450 recorded in remote montane snowpacks. Bulk snow ion concentrations were greatest in urban
 451 sites, but were not significantly different from nearby canyon sites located in protected areas,
 452 likely due to incursions of particulate-rich air. Concentrations of Na^+ and Cl^- were high and
 453 equivalent to maritime precipitation at all sites, due to the proximity of the Great Salt Lake.
 454 However, the impact of road salt application was evident even in this saline environment when
 455 concentrations spiked by an order of magnitude on protected montane sites to $\sim 3000 \mu\text{eq l}^{-1}$.
 456 Surface snow ion concentrations tracked temporal and spatial variation in atmospheric
 457 particulate concentrations, and were typically greatest at intermediate elevations (1400 – 1600

458 masl, or 100 – 300 m above the valley floor). Median N loading accompanying snowstorms
 459 measured 0.8 kg ha⁻¹ in January 2011, with additional contributions from dry/fog deposition that
 460 varied strongly with elevation. Wintertime anthropogenic air pollution and road salt application
 461 represent ecologically significant sources of nutrients and salts to the snowpack, with important
 462 implications for urban and adjacent ecosystems.

463

464 **Acknowledgements**

465 This project was inspired by S. Arens, whose research on ion deposition to the high elevation
 466 snowpack of the Wasatch Mountains provided a baseline for our study. We thank J. Horel, C. D.
 467 Whiteman, G. Silcox, and T. Cerling for discussion, D. Reim for snow depth measurements, and
 468 W. Brown from NCAR/EOL for providing the ceilometer. Funding was provided by the Funding
 469 Incentive Seed Grant Program at the University of Utah and by NSF grant ATM-0938397
 470 (PCAPS study). We thank the Utah Department of Air Quality for providing PM 2.5 data. This
 471 research was supported in part by NSF EPSCoR grant EPS 1208732 awarded to Utah State
 472 University, as part of the State of Utah Research Infrastructure Improvement Award. Any
 473 opinions, findings, and conclusions or recommendations expressed are those of the author(s) and
 474 do not necessarily reflect the views of the National Science Foundation.

475

476 **5. References**

477 Arens, S. J. T. 2010. Ion deposition in Wasatch Mountain snow: influence of Great Salt Lake and
 478 Salt Lake City. M. Sci. Thesis, University of Utah, Salt Lake City.

- 479 Baron, J. S., C. T. Driscoll, J. L. Stoddard, and E. E. Richer. 2011. Empirical critical loads of
 480 atmospheric nitrogen deposition for nutrient enrichment and acidification of sensitive US
 481 Lakes. *BioScience* 61:602–613.
- 482 Bergin, M. H., J.-L. Jaffrezo, C. I. Davidson, J. E. Dibb, S. N. Pandis, R. Hillamo, W. Maenhaut,
 483 H. D. Kuhns, and T. Makela. 1995. The contributions of snow, fog, and dry deposition to
 484 the summer flux of anions and cations at Summit, Greenland. *Journal of Geophysical*
 485 *Research: Atmospheres* 100:16275–16288.
- 486 Bettez, N. D., and P. M. Groffman. 2013. Nitrogen deposition in and near an urban ecosystem.
 487 *Environmental Science & Technology* 47:6047–6051.
- 488 Björkman, M.P., Kühnel, R., Partridge, D.G., Roberts, T.J., Aas, W., Mazzola, M., Viola, A.,
 489 Hodson, A., Ström, J., Isaksson, E., 2013. Nitrate dry deposition in Svalbard. *Tellus B*
 490 65:19071.
- 491 Cereceda-Balic, F., M. R. Palomo-Marín, E. Bernalte, V. Vidal, J. Christie, X. Fadic, J. L.
 492 Guevara, C. Miro, and E. Pinilla Gil. 2012. Impact of Santiago de Chile urban
 493 atmospheric pollution on anthropogenic trace elements enrichment in snow precipitation
 494 at Cerro Colorado, Central Andes. *Atmospheric Environment* 47:51–57.
- 495 Cerling, T. E., and A. J. Alexander. 1987. Chemical composition of hoarfrost, rime and snow
 496 during a winter inversion in Utah, U.S.A. *Water, Air, and Soil Pollution* 35:373–379.
- 497 Chen, A., J. G. Watson, J. C. Chow, M. C. Green, D. Inouye, and K. Dick. 2012. Wintertime
 498 particulate pollution episodes in an urban valley of the Western US: A case study.
 499 *Atmospheric Chemistry and Physics* 12:10051–10064.

- 500 Dolislager, L. J., R. VanCuren, J. R. Pederson, A. Lashgari, and E. McCauley. 2012. A summary
 501 of the Lake Tahoe Atmospheric Deposition Study (LTADS). *Atmospheric Environment*
 502 46:618–630.
- 503 Fenn, M. E., R. Haeuber, G. S. Tonnesen, J. S. Baron, S. Grossman-Clarke, D. Hope, D. A. Jaffe,
 504 S. Copeland, L. Geiser, H. M. Rueth, and J. O. Sickman. 2003. Nitrogen emissions,
 505 deposition, and monitoring in the western United States. *Bioscience* 53:391–403.
- 506 Gatz, D. F. 1991. Urban precipitation chemistry: A review and synthesis. *Atmospheric*
 507 *Environment. Part B. Urban Atmosphere* 25:1–15.
- 508 Hand, J. L., B. A. Schichtel, M. Pitchford, W. C. Malm, and N. H. Frank. 2012. Seasonal
 509 composition of remote and urban fine particulate matter in the United States. *Journal of*
 510 *Geophysical Research D: Atmospheres* 117.
- 511 Jeffries, D. S. 1990. Snowpack storage of pollutants, release during melting, and impact on
 512 receiving waters. Pages 107–132 in S. A. Norton, S. E. Lindberg, and A. L. Page, editors.
 513 *Acidic Precipitation*. Springer New York.
- 514 Kang, S., P. a Mayewski, D. Qin, S. a Sneed, J. Ren, and D. Zhang. 2004. Seasonal differences
 515 in snow chemistry from the vicinity of Mt. Everest, central Himalayas. *Atmospheric*
 516 *Environment* 38:2819–2829.
- 517 Karraker, N. E., J. P. Gibbs, and J. R. Vonesh. 2008. Impacts of road deicing salt on the
 518 demography of vernal pool-breeding amphibians. *Ecological Applications* 18:724–734.
- 519 Kelly, K. E., R. Kotchenruther, R. Kuprov, and G. D. Silcox. 2013. Receptor model source
 520 attributions for Utah’s Salt Lake City airshed and the impacts of wintertime secondary
 521 ammonium nitrate and ammonium chloride aerosol. *Journal of the Air & Waste*
 522 *Management Association* 63:575–590.

- 523 Lajtha, K., and J. Jones. 2013. Trends in cation, nitrogen, sulfate and hydrogen ion
 524 concentrations in precipitation in the United States and Europe from 1978 to 2010: a new
 525 look at an old problem. *Biogeochemistry* 116:303–334.
- 526 Lareau, N. P., E. Crosman, C. D. Whiteman, J. D. Horel, S. W. Hoch, W. O. J. Brown, and T. W.
 527 Horst. 2013. The persistent cold-air pool study. *Bulletin of the American Meteorological*
 528 *Society* 94:51–63.
- 529 Lewis, J. E., T. R. Moore, and N. J. Enright. 1983. Spatial-temporal variations in snowfall
 530 chemistry in the montreal region. *Water, Air, and Soil Pollution* 20:7–22.
- 531 Lewis, W. M., M. C. Grant, and J. F. Saunders. 1984. Chemical patterns of bulk atmospheric
 532 deposition in the state of Colorado. *Water Resources Research* 20:1691–1704.
- 533 Lovett, G. M., M. M. Traynor, R. V. Pouyat, M. M. Carreiro, W.-X. Zhu, and J. W. Baxter.
 534 2000. Atmospheric deposition to oak forests along an urban–rural gradient.
 535 *Environmental Science & Technology* 34:4294–4300.
- 536 Molotch, N. P., and R. C. Bales. 2005. Scaling snow observations from the point to the grid
 537 element: Implications for observation network design. *Water Resources Research*
 538 41:W11421.
- 539 Nickus, U., M. Kuhn, U. Baltensperger, R. Delmas, H. Gäggeler, A. Kasper, H. Kromp-Kolb, F.
 540 Maupetit, A. Novo, F. Pichlmayer, S. Preunkert, H. Puxbaum, G. Rossi, W. Schöner, M.
 541 Schwikowski, P. Seibert, M. Staudinger, V. Trockner, D. Wagenbach, and W.
 542 Winiwarter. 1997. SNOSP: Ion deposition and concentration in high alpine snow packs.
 543 *Tellus B* 49:56–71.
- 544 Pinheiro, J., D. Bates, S. DebRoy, D. Sarkar, and R Core Development Team. 2013. nlme:
 545 Linear and Nonlinear Mixed Effects Models.

- 546 Pomeroy, J. W., T. D. Davies, H. G. Jones, P. Marsh, N. E. Peters, and M. Tranter. 1999.
 547 Transformations of snow chemistry in the boreal forest: accumulation and volatilization.
 548 Hydrological Processes 13:2257–2273.
- 549 Rao, P., L. R. Hutyra, S. M. Raciti, and P. H. Templer. In press. Atmospheric nitrogen inputs and
 550 losses along an urbanization gradient from Boston to Harvard Forest, MA.
 551 Biogeochemistry:1–17.
- 552 Silcox, G. D., K. E. Kelly, E. T. Crosman, C. D. Whiteman, and B. L. Allen. 2012. Wintertime
 553 PM_{2.5} concentrations during persistent, multi-day cold-air pools in a mountain valley.
 554 Atmospheric Environment 46:17–24.
- 555 Wallace, J., and P. Kanaroglou. 2009. The effect of temperature inversions on ground-level
 556 nitrogen dioxide (NO₂) and fine particulate matter (PM_{2.5}) using temperature profiles
 557 from the Atmospheric Infrared Sounder (AIRS). Science of The Total Environment
 558 407:5085–5095.
- 559 Whiteman, C.D., Hoch, S.W., Horel, J.D., Charland, A., 2014. Relationship between particulate
 560 air pollution and meteorological variables in Utah’s Salt Lake Valley. Atmos. Environ.
 561 94, 742–753.
- 562 Williams, M. W., and J. M. Melack. 1991. Precipitation chemistry in and ionic loading to an
 563 alpine basin, Sierra Nevada. Water Resources Research 27:1563–1574.
- 564 Williams, M. W., C. Seibold, and K. Chowanski. 2009. Storage and release of solutes from a
 565 subalpine seasonal snowpack: soil and stream water response, Niwot Ridge, Colorado.
 566 Biogeochemistry 95:77–94.
- 567 Williams, M. W., and K. A. Tonnessen. 2000. Critical loads for inorganic N deposition in the
 568 Colorado Front Range, USA. Ecological Applications 10:1648–1665.

569 Yalcin, K., C. P. Wake, J. E. Dibb, and S. I. Whitlow. 2006. Relationships between aerosol and
570 snow chemistry at King Col, Mt. Logan Massif, Yukon, Canada. *Atmospheric*
571 *Environment* 40:7152–7163.

572

573

574 **Tables**

575 Table 1: Comparison of mean ion concentrations ($\mu\text{eq l}^{-1}$ with standard deviations in parentheses) in snow samples measured in
 576 several previous studies in the Western United States. Wasatch samples represent peak snowpack full column concentrations in 2009
 577 from 16 high-elevation locations in the Wasatch Mountains, Utah (Arens 2010). Niwot Ridge is an alpine tundra site in the Rocky
 578 Mountains near Boulder, Colorado; concentrations represent snowpack from 2006 - 7 (Williams et al. 2009). Emerald Lake is in the
 579 Southern Sierra Nevada Mountains in California, samples represent cumulative snowfall from 1985 – 88 (Williams and Melack 1991).
 580 Urban samples from Montreal, Canada were collected in 1980 (Lewis et al. 1983). Samples from sites in Salt Lake City represent
 581 mean ion concentrations in rime, surface hoar, and surface snow during a persistent cold air pool in 1985-86 (Cerling and Alexander
 582 1987). Salt Lake City bulk snow ion concentrations are from the present study.

583

Location	Elevation (m)	Cl ⁻	NO ₃ ⁻	SO ₄ ²⁻	NH ₄ ⁺	K ⁺	Na ⁺	Mg ²⁺	Ca ²⁺
Wasatch Mountains (Utah)	2050 – 3050	40.4 (13)	7.5 (1)	20.5 (5.2)	11.6 (2.6)	7.1 (4.7)	43.6 (15.1)	10.3 (3.3)	57.9 (21.2)
Rocky Mountains (Niwot Ridge, Colorado)	3340	1.7	11.5	7.0	4.5	3.6	2.0	4.2	22.6
Sierra Nevada Mountains (Emerald Lake, California)	2800 - 3400	2.8	2.3	2.0	1.7	0.7	1.3	0.6	1.3
Montreal, Canada (1980)	10 - 40	114 (88)	35 (12)	63 (56)	10 (8)	21 (19)	103 (99)	11 (7)	68 (93)
Salt Lake City (1985-6)	1400	1910	1260	1160	1690	60	1690	240	1220

Salt Lake City bulk snow (this study)	1300 - 1400	117 (118)	39 (35)	25 (33)	42 (43)	3 (3)	120 (124)	11 (8)	36 (26)
--	-------------	-----------	---------	---------	---------	-------	-----------	--------	---------

584 Table 2: Pairwise (Pearson) correlation coefficients among ion concentrations in bulk snow
 585 samples (a) and snow surface samples (b). Significant correlations ($p < 0.05$) are denoted by
 586 bold-face type.

a)	Bulk snow samples								
	H ⁺	NH ₄ ⁺	Ca ²⁺	Mg ²⁺	Na ⁺	K ⁺	Cl ⁻	NO ₃ ⁻	SO ₄ ²⁻
H ⁺	1								
NH ₄ ⁺	-0.4	1							
Ca ²⁺	-0.5	0.59	1						
Mg ²⁺	-0.46	0.71	0.92	1					
Na ⁺	-0.21	0.88	0.58	0.73	1				
K ⁺	-0.2	0.45	0.55	0.57	0.45	1			
Cl ⁻	-0.22	0.7	0.58	0.73	1	0.45	1		
NO ₃ ⁻	-0.29	0.94	0.57	0.56	0.74	0.37	0.58	1	
SO ₄ ²⁻	-0.35	0.92	0.66	0.7	0.86	0.34	0.85	0.83	1

b)	Snow surface samples								
	H ⁺	NH ₄ ⁺	Ca ²⁺	Mg ²⁺	Na ⁺	K ⁺	Cl ⁻	NO ₃ ⁻	SO ₄ ²⁻
H ⁺	1								
NH ₄ ⁺	0.02	1							
Ca ²⁺	-0.78	0.75	1						
Mg ²⁺	-0.7	0.7	0.72	1					
Na ⁺	-0.33	0.26	0.32	0.69	1				
K ⁺	0.07	0.44	0.31	0.44	0.49	1			
Cl ⁻	-0.35	0.47	0.32	0.69	1	0.48	1		
NO ₃ ⁻	0.54	0.76	0.73	0.77	0.57	0.27	0.63	1	
SO ₄ ²⁻	0.6	0.82	0.96	0.69	0.41	0.4	0.61	0.79	1

587
 588
 589
 590
 591
 592
 593
 594

595 **Figure captions**

596 **Figure 1:** Sampling locations in the Salt Lake Valley metropolitan area and adjacent Wasatch
 597 Mountains. Panel b) is enlarged from the box in panel a). Diamonds, pluses, and x marks denote
 598 stormboards in Red Butte Canyon, Big Cottonwood Canyon, and urban sites, respectively.
 599 Squares and circles denote urban and montane elevation transects. The triangle represents the
 600 laser ceilometer.

601
 602 **Figure 2:** Images of cold air pools and associated high aerosol concentrations in the Salt Lake
 603 Valley. At left is a view of the cold-air pool on January 7, 2011, looking from the montane
 604 elevation gradient across the urban area. At right is a photo of a cold-air pool on Dec. 18, 2011,
 605 penetrating into Mill Creek Canyon in the Wasatch Mountains adjacent to the Salt Lake Valley.

606
 607 **Figure 3:**
 608 Ion concentrations in bulk snow samples plotted by sites ranked according to elevation on the
 609 ordinate. Boxes represent medians and the interquartile range; data > 1.5 times the range from
 610 the box to the whiskers are denoted as outliers (circles). “Urban” denotes samples from three
 611 urban locations; low, mid, high, and very-high prefixes represent elevations in Red Butte (RB)
 612 and Big Cottonwood (BC) canyons, respectively. Sites with different lowercase letters were
 613 significantly different (Tukey comparison, $p < 0.05$). An outlier with a Cl^- concentration of 2140
 614 $\mu\text{eq l}^{-1}$ in an urban sample was omitted for clarity.

615
 616 **Figure 4:** Daily mean concentrations of particulate matter (PM 2.5, black line) and snow surface
 617 ion concentrations plotted by date during January 2011 for the urban (red) and montane (blue)

618 elevation transects. The U. S. EPA national ambient air quality standard is $35 \mu\text{g m}^{-3}$ (24 hr
 619 mean). Grey shaded areas represent time-integrated PM 2.5 exposure of surface snow between
 620 the prior snow precipitation event and a given sampling date. Ion concentrations were
 621 significantly greater on either January 7, or both January 7 and 30, as compared with January 14
 622 or 24 for several ions (Cl^- , Na^+ , Ca^{2+} , K^+) in the montane transect. Concentrations of Ca^{2+} , NO_3^- ,
 623 and SO_4^{2-} in the urban transect were significantly greater on January 28 than the other sampling
 624 dates (January 5, 14, 24, and 26). Temporal trends in Na^+ , Mg^{2+} , SO_4^{2-} , and K^+ are shown in Fig
 625 A3.

626
 627 **Figure 5:** Time-height cross-section of aerosol backscatter (\log_{10} of backscatter coefficient β in
 628 $\text{m}^{-1} \text{sr}^{-1}$), measured with a laser ceilometer. Brighter colors (reds) indicate regions and periods of
 629 increased backscatter (more positive β) as indicated in the legend. Precipitation events are
 630 indicated by vertical dashed lines with new snow accumulation totals (measured near the mouth
 631 of Little Cottonwood Canyon) given on top of the figure. Time intervals between snow
 632 precipitation and surface snow sampling events are denoted by blue and red lines below the
 633 figure for the montane and urban transects, respectively.

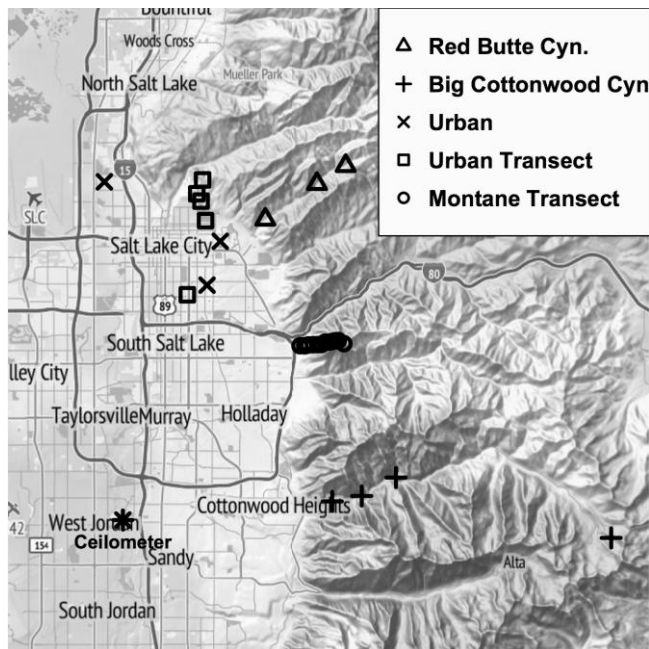
634
 635 **Figure 6:** Snow surface ion concentrations by elevation and sampling date during January 2011
 636 for the urban (red) and montane (blue) elevation transects. Different symbols denote different
 637 sampling dates. Sodium and Cl^- concentrations were an order of magnitude higher on January 7
 638 than other dates (see insets with distinct scales). Ion concentrations decreased with elevation in
 639 the montane transect according to trends that significantly differed among sampling dates. Ion

640 concentrations generally did not covary with elevation in the urban transects, but NH_4^+ and NO_3^-
 641 showed significant non-linear elevational trends on January 28.

642
 643 **Figure 7:** Daily average near-surface air temperatures, aerosol exposure index (see Methods),
 644 and surface snow NH_4^+ and NO_3^- concentrations as a function of elevation during late January
 645 2011 (dates shown in the legends). The top panels represent two dates with relatively unstable
 646 atmospheric conditions, when temperatures decreased at approximately $5.5 \text{ }^\circ\text{C km}^{-1}$ (dotted lines,
 647 left panels), and snow surface ions showed little relationship with elevation. The bottom panels
 648 illustrate dates with a strong temperature inversion between 1600 – 2000 masl, leading to
 649 increased aerosol exposure and snow surface N concentrations.

650
 651
 652
 653
 654
 655
 656
 657
 658
 659
 660
 661
 662

663 Figure 1:



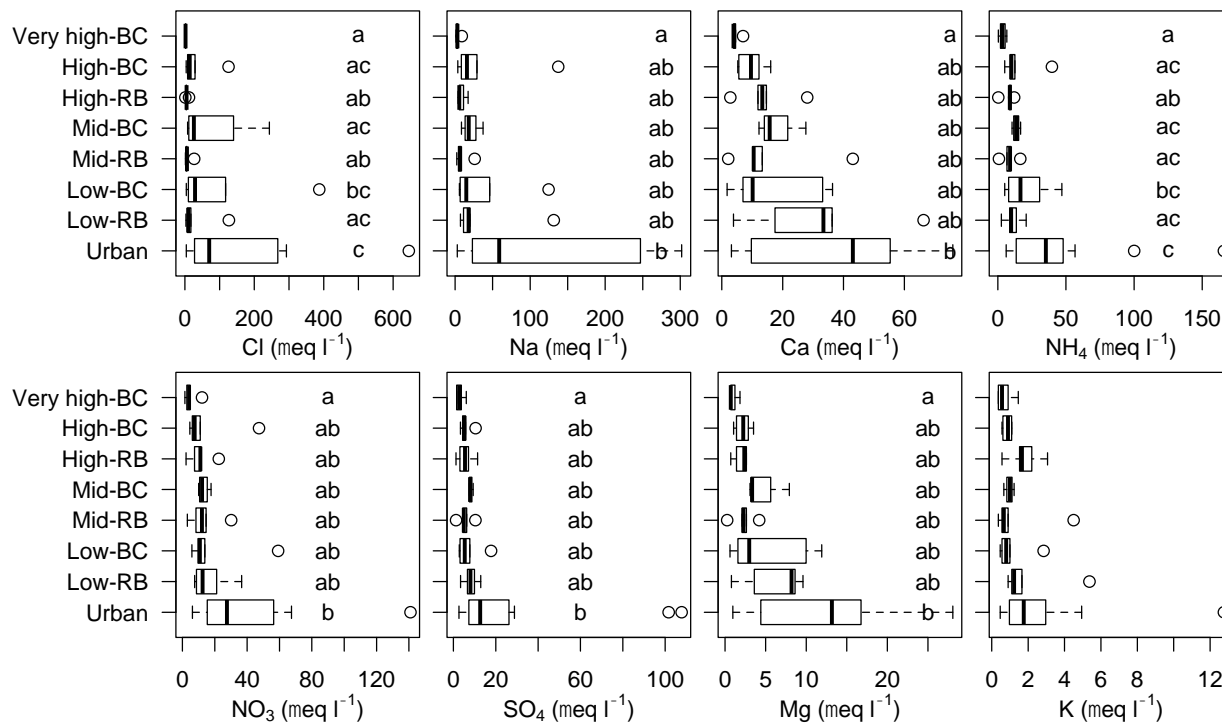
664
665
666
667
668
669
670
671
672
673
674
675
676
677
678
679
680
681
682
683
684
685
686
687
688
689
690
691

692 Figure 2
693



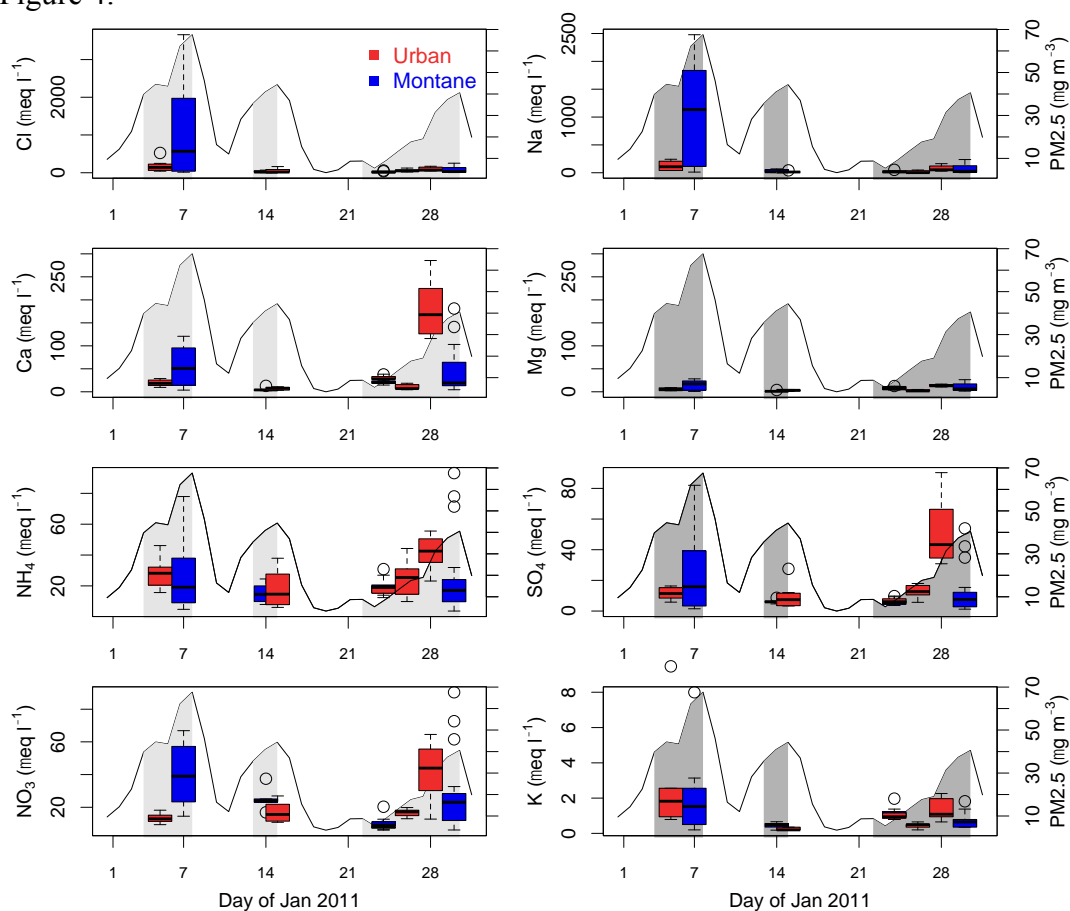
694
695
696
697
698
699
700
701

702 Figure 3:
703
704



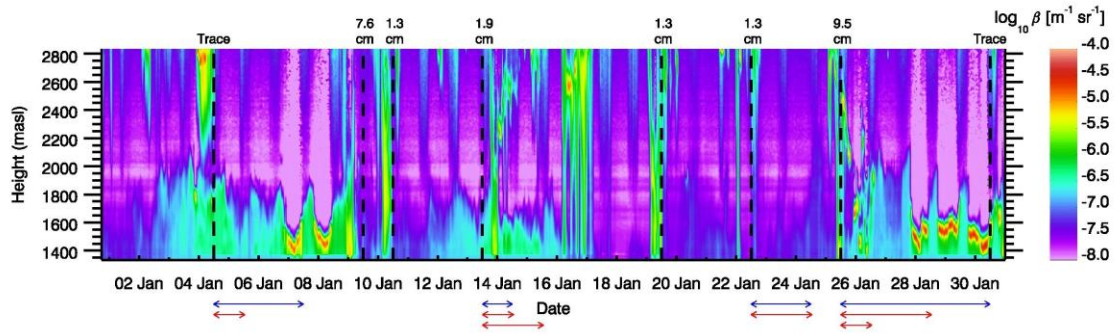
705
706
707
708

709 Figure 4:



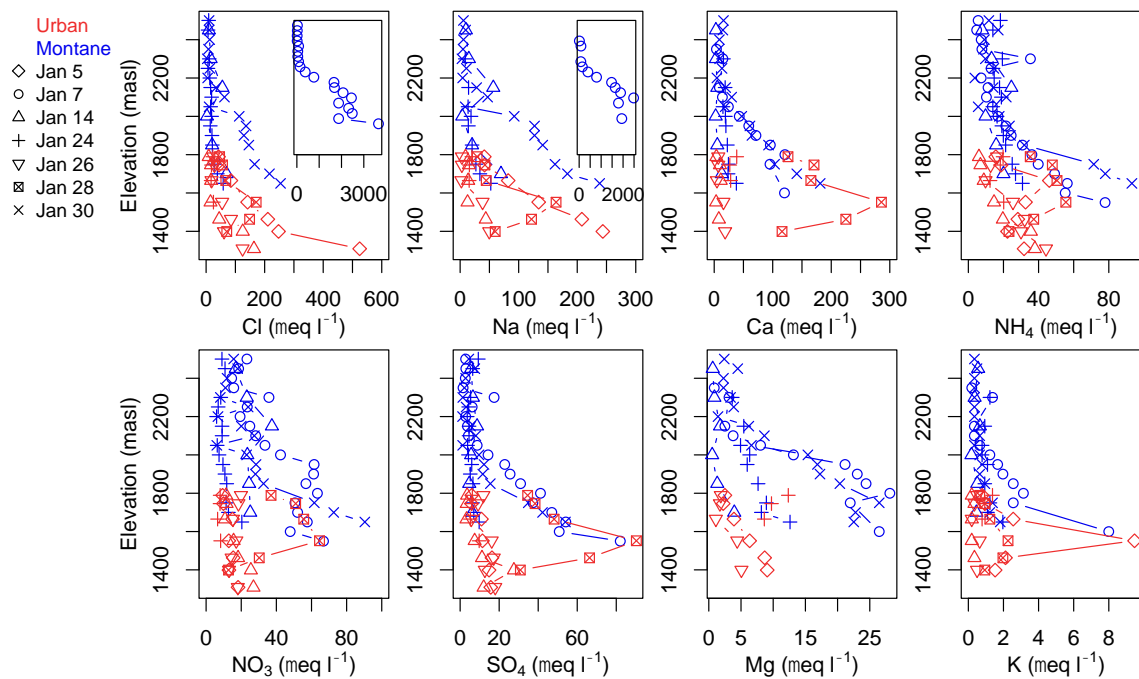
710
711
712

713 Figure 5:
714



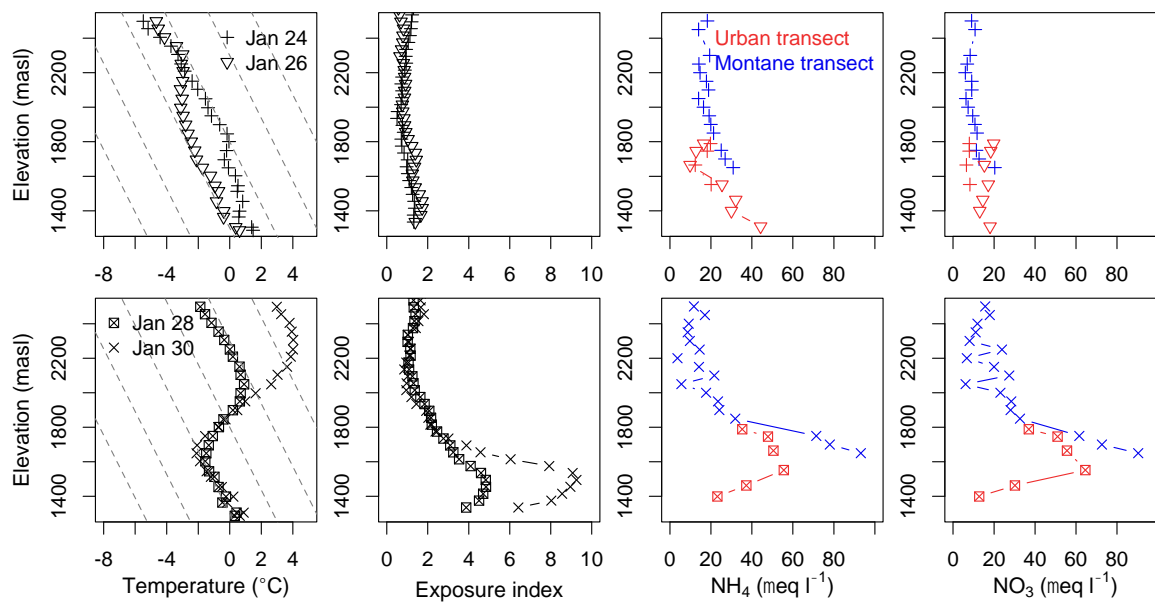
715
716
717

718 Figure 6:
719



720
721
722
723
724

725 Figure 7:



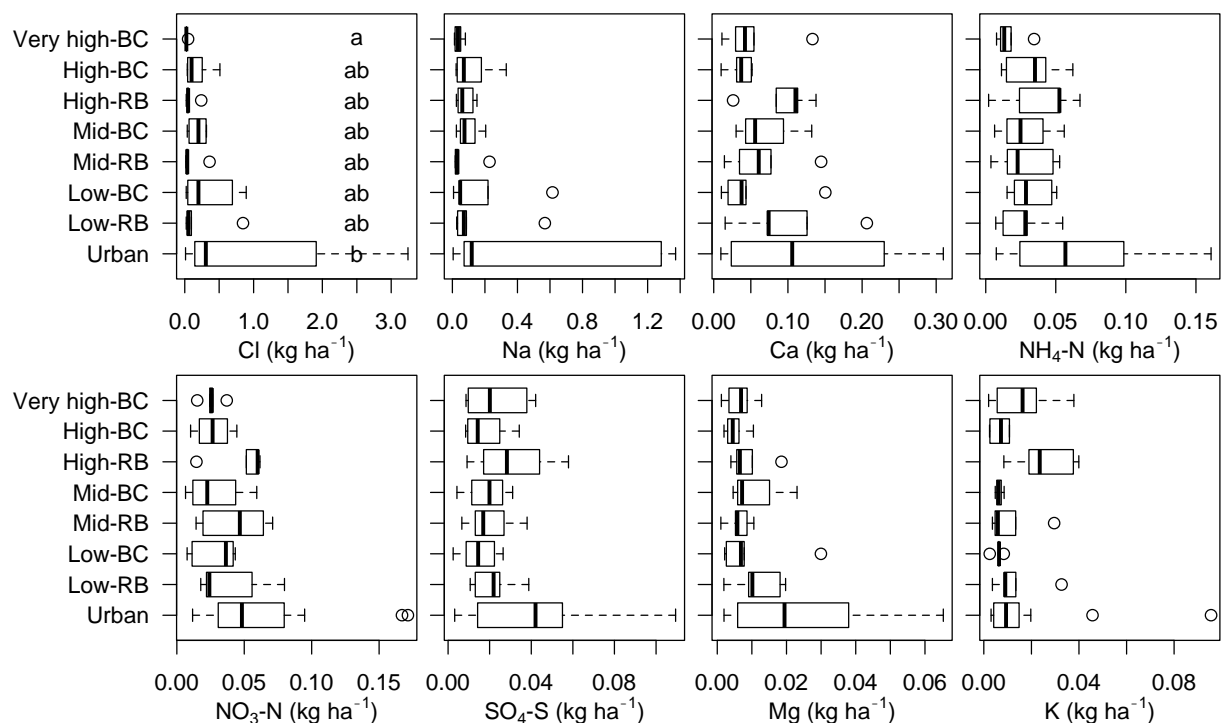
726
727
728

729 **Appendix A**

730 Figure A1:

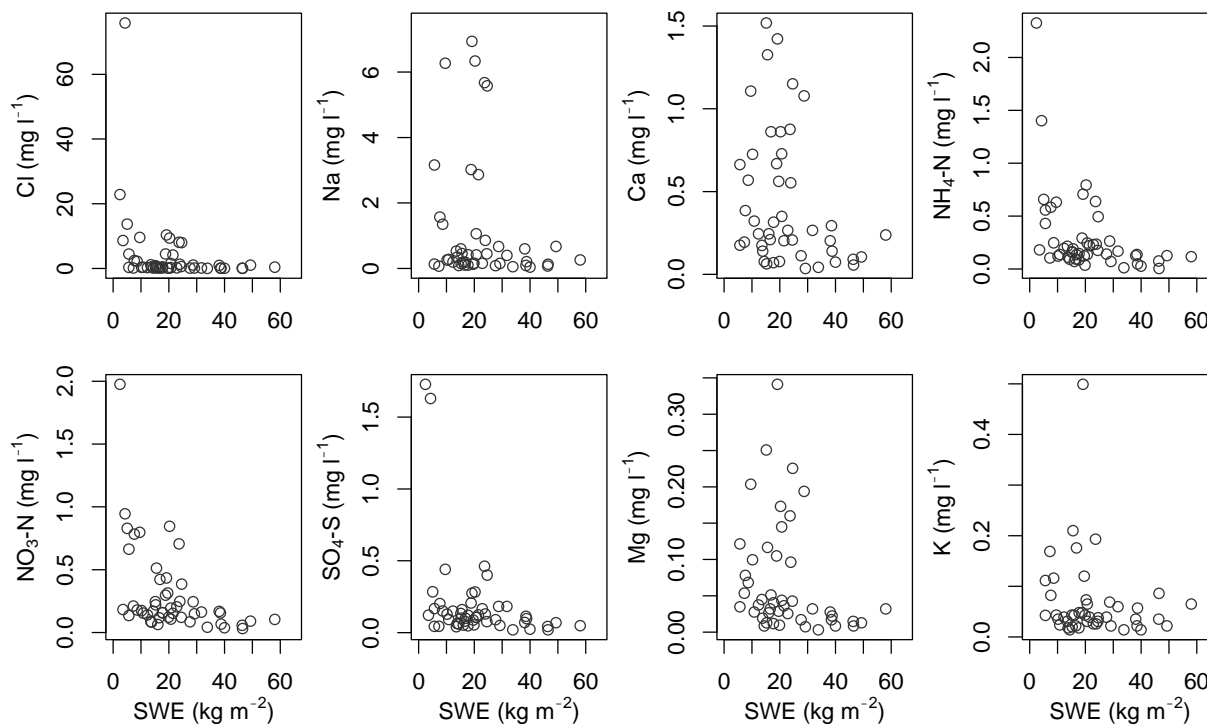
731 Ion loading (the product of ion concentrations and snow water equivalent) in bulk snow samples
 732 by site arranged by elevation on the ordinate. Each datum represents an individual snow
 733 precipitation event. Boxes represent medians and the interquartile range; data > 1.5 times the
 734 range from the box to the whiskers are denoted as outliers (circles). Urban denotes samples from
 735 three urban locations, and low, mid, high, and very-high prefixes represent site elevation in Red
 736 Butte (RB) and Big Cottonwood (BC) canyons, respectively.

737
738



739
740
741

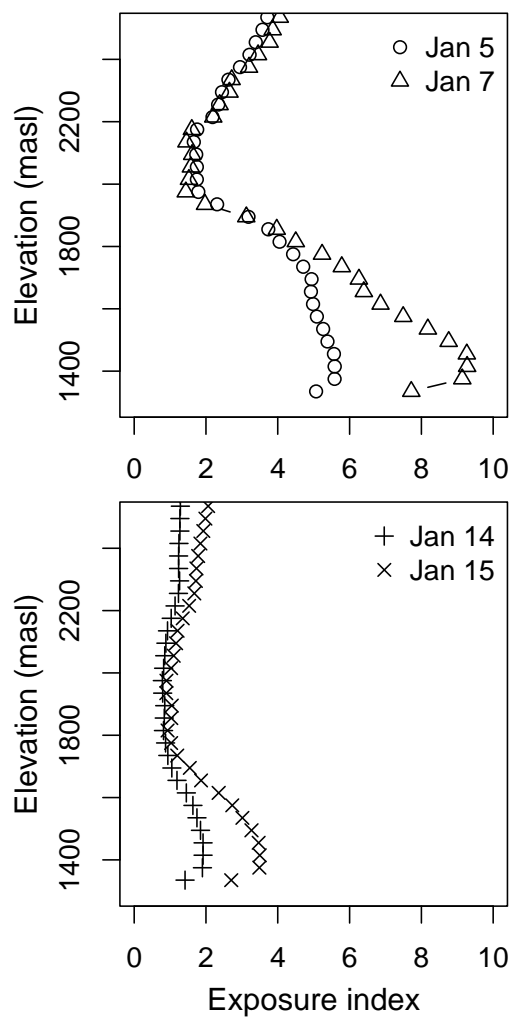
742 Figure A2:
743 Relationships between ion concentrations and snow water equivalent (SWE) in the bulk snow
744 samples.



745
746
747
748
749
750
751
752
753
754
755
756

757 Figure A3: Patterns of aerosol exposure (see Methods) plotted by elevation and time during the
 758 development of two cold air pools (top and bottom panels) in January 2011. Different symbols
 759 represent different dates as indicated in the legends.

760



761
762